Paper:

Biologically-Inspired Locomotion Controller for a Quadruped Walking Robot:
Analog IC Implementation of a CPG-Based Controller

Kazuki Nakada, Tetsuya Asai, and Yoshihito Amemiya

Department of Electrical Engineering, Hokkaido University
Kita 13 Nishi 8, Sapporo 060-8628, Japan
E-mail: nakada@sapiens-ei.eng.hokudai.ac.jp
[Received January 3, 2004; accepted June 23, 2004]

The present paper proposes analog integrated circuit (IC) implementation of a biologically inspired controller in quadruped robot locomotion. Our controller is based on the central pattern generator (CPG), which is known as the biological neural network that generates fundamental rhythmic movements in locomotion of animals. Many CPG-based controllers for robot locomotion have been proposed, but have mostly been implemented in software on digital microprocessors. Such a digital processor operates accurately, but it can only process sequentially. Thus, increasing the degree of freedom of physical parts of a robot deteriorates the performance of a CPG-based controller. We therefore implemented a CPG-based controller in an analog complementary metal-oxide-semiconductor (CMOS) circuit that processes in parallel essentially, making it suitable for real-time locomotion control in a multi-legged robot. Using the simulation program with integrated circuit emphasis (SPICE), we show that our controller generates stable rhythmic patterns for locomotion control in a quadruped walking robot, and change its rhythmic patterns promptly.

Keywords: biologically-inspired approach, locomotion, central pattern generator, analog IC implementation

1. Introduction

Biologically inspired approaches have recently succeeded in locomotion control in robotics [1]. Biological systems have been evolved to optimize themselves under selective pressures for a long time. Therefore, biological findings are expected to provide with us innovative ideas in design and control methods in robotics.

Central pattern generators (CPGs) are the biological neural networks that can generate fundamental rhythmic movements in locomotion of animals, such as walking, running, swimming, and flying. Such rhythmic movements induce coordination of physical parts [2]. Since the degree of freedom (DOF) relevant to locomotion is very high, such coordination is necessary for stable locomotion. Thus, CPG plays a significant role in locomotion of animals.

Many researchers have applied the concept of CPG to control walking robots [4–8]. Kimura et al. developed the quadruped robot, *Tekken*, adapts to irregular terrain using CPG dynamics [4]. Billard and Ijspeert implemented a CPG controller in a quadruped robot [5], and Lewis et al. designed and fabricated an analog CPG chip for a biped robot [7]. Such approaches to locomotion control reduce the amount of calculation required for motion control because they do not need complicated planning to generate a motion trajectory, and adapt well to unexpected disturbance because a CPG interacts with environments through sensory information [7].

Focusing on such advantages, we propose hardware implementation of a CPG-based controller for rhythmic coordination in quadruped robot locomotion. Previously proposed CPG-based locomotion controllers have mostly been implemented in software on digital microprocessors. Such a digital processor operates accurately, but processes only sequentially, deteriorating controller performance as the DOF of physical components in a robot increases. We therefore designed a CPG-based controller as an analog integrate circuit (IC) that processes in parallel essentially. We previously proposed analog IC implementation of a CPG-based controller for a quadruped robot [12]. Our previous controller operates through current interaction, and thus it is difficult to operate stably without precise tuning of bias currents [12]. In contrast, the controller we propose here operates through voltage interaction, reducing bias currents and stabilizing operation. Using the simulation program with integrated circuit emphasis (SPICE), we show that our CPG-based controller generates desired rhythmic patterns for locomotion control in a quadruped walking robot.

This paper is divided into five sections. In Section 2, we propose a CPG-based locomotion controller for a quadruped walking robot. In Section 3, we describe an analog IC implementation of the proposed controller. In Section 4, we confirm the desired operation of the circuit as a CPG-based controller through circuit simulations. In Section 5, we summarize our work.

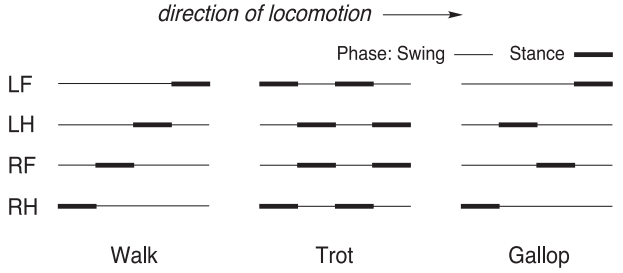

Fig. 1. Phase diagrams of typical locomotion patterns of mammals. (a) Walk, (b) Trot, and (c) Gallop.

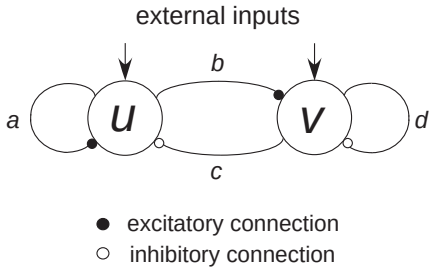

Fig. 2. Configurations of the Wilson-Cowan neural oscillators.

2. CPG Controller

In this section, we propose a CPG-based controller for interlimb coordination in quadruped locomotion.

2.1. Biological Principles of Locomotion of Animals

Firstly, let us briefly review the biological principles in locomotion control of animals. Locomotion of animals, such as walking, running, swimming, and flying is based on rhythmic movements. Such rhythmic movements are generated by the biological neural network known as the central pattern generator (CPG) [2]. CPG consists of sets of neural oscillators, situated in the ganglion or spinal cord. Induced by inputs from command neurons, CPG generates a rhythmic pattern of neural activity voluntary. Such a rhythmic pattern activates motor neurons and, in turn, a rhythmic movement of animals [3].

In locomotion of animals, one of the fundamental roles of CPG is controlling of each of the limbs. As a result of interaction with CPGs that actuate muscles at each joint of the limbs, rhythmic movements of each of the limbs are stabilized. Another one is cooperation between the limbs, i.e., interlimb coordination. CPGs that control each of the limbs are synchronized via coordinating interneurons, and thus the interlimb coordination is achieved. Since the DOF of physical parts relevant to locomotion is very high, physical coordination, such as interlimb coordination, is required for stable locomotion. Rhythmic movements generated by CPGs induces this coordination. Thus, CPG can be said to play a central role in locomotion of animals.

Locomotion patterns of animals are characterized by phase relationship in limb movements. In other words, it is considered as phase-locked oscillation of the limbs. **Fig.1** shows typical locomotion patterns of mammals, such as the walk, trot and gallop. LF, LH, RF, and RH represent the left forelimb, left hindlimb, right forelimb, and right hindlimb. Bold lines and thin lines represent stance phases and swing phases during locomotion.

2.2. CPG Model for Interlimb Coordination

Among the many CPG models [9–11], most are constructed using a set of coupled neural oscillators, each controlling a joint of the limb. We constructed a CPG model from the Wilson-Cowan neural oscillator [13], consisting of excitatory and inhibitory neurons with synaptic connections (**Fig.2**). The dynamics of the Wilson-Cowan neural oscillator is expressed by the following equations:

$$\tau_u \frac{du}{dt} = -u + f_\mu(au - bv + s_u) \quad \ldots\ldots \quad (1)$$

$$\tau_v \frac{dv}{dt} = -v + f_\mu(cu - dv + s_v) \quad \ldots\ldots \quad (2)$$

where u and v express the activity of a group of excitatory and inhibitory neurons, parameters a through d coupling strength between the groups of neurons, s_u and s_v external inputs, and τ_u and τ_v time constants. Transfer function $f_\mu(x)$ is given by the hyperbolic tangent $\tanh(\mu x)$, where μ is the control parameter. Depending on the parameters, the Wilson-Cowan neural oscillator shows various behaviors, such as a limit-cycle oscillation. Many researchers have investigated its dynamics in detail [13–15].

By coupling the Wilson-Cowan neural oscillators, we constructed a CPG network model for rhythmic interlimb coordination in quadruped locomotion. The dynamics of the model is expressed by the following equations [13]:

$$\frac{du_i}{dt} = -u_i + f_\mu\left(\sum_j a_{ij}u_j - \sum_j b_{ij}v_j + s_{u_i}\right) \quad .. \quad (3)$$

$$\frac{dv_i}{dt} = -v_i + f_\mu\left(\sum_j c_{ij}u_j - \sum_j d_{ij}v_j + s_{v_i}\right) \quad .. \quad (4)$$

where a_{ij} through d_{ij} express coupling strength between groups of neurons. As a CPG network model for rhythmic interlimb coordination, it is desirable to generate various rhythmic patterns. This network model can generate different phase-locked oscillation according to its coupling configuration.

3. Circuit Implementation

We here describe an analog complementary metal-oxide-semiconductor (CMOS) circuit implementation of the CPG-based controller. In our previous work, we proposed an analog CMOS circuit implementing a CPG-based controller for quadruped robotic locomotion [12]. The previous circuit operates through current interaction, and thus it is difficult to operate stably without precise tuning of bias currents. To reduce bias currents for stable

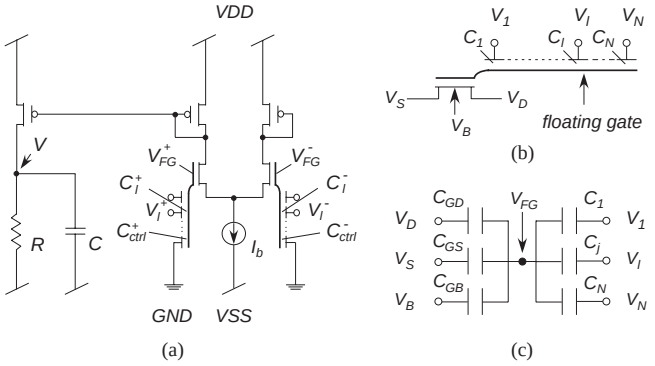

Fig. 3. Schematic of cell circuit.

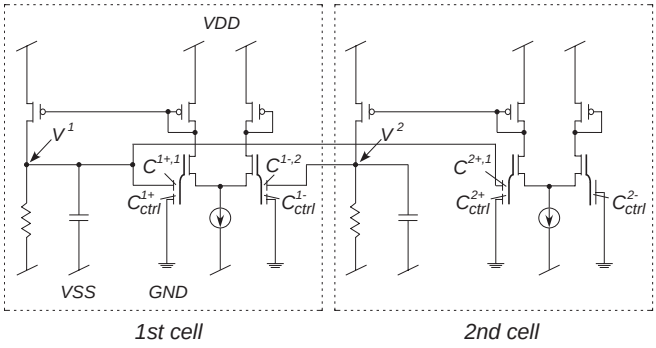

Fig. 4. Schematic of unit circuit.

operation, we propose a novel analog CMOS circuit that operates through voltage interaction.

3.1. Cell Circuit

First, we describe a cell circuit that constitutes a part of the CPG controller. The cell circuit consists of four analog elementary circuits, a differential pair, a current mirror, an RC circuit and a current source (**Fig.3(a)**).

The differential pair, the most fundamental components of the cell circuit, approximates the nonlinearity of the transfer function. When MOS transistors comprising the differential pair operate in weak inversion region, the static response of the differential pair is represented as [16]:

$$I_\mu(V^+ - V^-) = I_b \frac{1+\tanh(\mu(V^+ - V^-))}{2} \quad \ldots \quad (5)$$

where I_μ is the output current of the differential pair, V^+ and V^- the input voltages, I_b the bias current, $\mu = \kappa/2V_T$, V_T the thermal voltage, and κ the effectiveness of the gate potential. By subtracting a half of the bias current from the output current I_μ, we derive transfer function $f_\mu(x)$.

We replace the MOS transistors comprising the differential pair with multiple-input floating-gate (MIFG) MOS transistors [19, 20] (**Fig.3(b)**), aiming at the operation of weighted linear summation of voltages. The floating-gate voltage of the MIFG MOS transistor is expressed by the following equation [19]:

$$V_{\mathrm{FG}} = \frac{C_{\mathrm{GD}}}{C_{\mathrm{T}}}V_{\mathrm{D}} + \frac{C_{\mathrm{GS}}}{C_{\mathrm{T}}}V_{\mathrm{S}} + \frac{C_{\mathrm{GB}}}{C_{\mathrm{T}}}V_{\mathrm{B}} + \frac{Q_0}{C_{\mathrm{T}}} + \sum_l^N \frac{C_l}{C_{\mathrm{T}}}V_l \quad (6)$$

where V_l is the l-th input gate voltage; C_l the capacitance between each of the input gates and the floating-gate; V_{D}, V_{S}, and V_{B} the voltage of drain, source, and bulk; and Q_0 an initial charge in the floating-gate. Total capacitance of the floating-gate is expressed by:

$$C_{\mathrm{T}} = C_{\mathrm{GD}} + C_{\mathrm{GS}} + C_{\mathrm{GB}} + \sum_l^N C_l \quad \ldots \quad (7)$$

where C_{GD}, C_{GS}, and C_{GB} are the capacitance between the floating-gate and drain, source and bulk (**Fig.3(c)**). The floating-gate voltage is approximately expressed by [20]:

$$V_{\mathrm{FG}} \simeq \sum_l^N \frac{C_l}{C_{\mathrm{T}}}V_l \quad \ldots \quad (8)$$

where it is assumed that Q_0 is 0 and $C_{\mathrm{GD}}, C_{\mathrm{GS}}, C_{\mathrm{GB}} \ll C_{\mathrm{T}}$. The differential voltage between the floating-gates of the differential pair with MIFG MOS transistors is approximately expressed by the following equation:

$$V^+_{\mathrm{FG}} - V^-_{\mathrm{FG}} \simeq \sum_l^N \frac{C^+_l}{C_{\mathrm{T}}}V^+_l - \sum_l^N \frac{C^-_l}{C_{\mathrm{T}}}V^-_l \quad \ldots \quad (9)$$

where V^+_{FG} and V^-_{FG} are floating-gate voltages, V^+_l and V^-_l input gate voltages, and C^+_l and C^-_l capacitances between each input gate and the floating-gate.

After the output current of the differential pair with MIFG MOS transistors is reversed by the current mirror, it is integrated by the RC circuit. The circuit dynamics is expressed by the following equation:

$$C\dot{V} = -\frac{V - V_{\mathrm{SS}}}{R} + I_\mu(V^+_{\mathrm{FG}} - V^-_{\mathrm{FG}}) \quad \ldots \quad (10)$$

where C is capacitance and R resistance. For setting the equilibrium voltage at zero, we set substrate voltage $V_{\mathrm{SS}} < 0$ and $V_{\mathrm{SS}}/R + I_b/2 = 0$. The equation above is then rewritten as follows:

$$\begin{aligned} C\dot{V} &= -\frac{V}{R} + \frac{I_b}{2}\tanh(\mu(V^+_{\mathrm{FG}} - V^-_{\mathrm{FG}})) \\ &\simeq -\frac{V}{R} + \frac{I_b}{2}\tanh\left(\mu\left(\sum_l \frac{C^+_l}{C_{\mathrm{T}}}V^+_l - \sum_l \frac{C^-_l}{C_{\mathrm{T}}}V^-_l\right)\right) \\ &= -\frac{V}{R} + \frac{I_b}{2}F_\mu\left(\sum_l C^+_l V^+_l - \sum_l C^-_l V^-_l\right) \quad \ldots \quad (11) \end{aligned}$$

where we have replaced $F_\mu(x) = \tanh(\mu x/C_{\mathrm{T}})$.

Figure 4 shows a unit circuit that consists of two cell circuits, where V^1 and V^2 represent the volatege of the first and the second cell. This unit circuit has reciprocal interaction via capacitive coupling. The stability of the equilibrium point in the circuit is attained by adjusting all physical parameters. If the equilibrium point is unstable and the system is not divergent, the unit circuit generates periodic patterns autonomously.

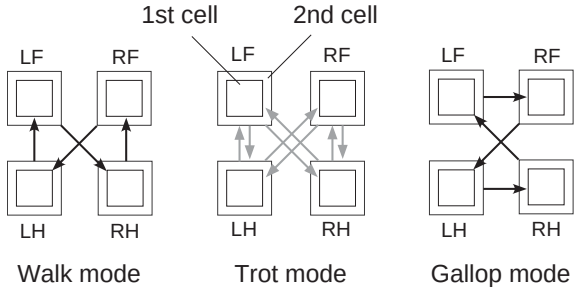

Fig. 5. Coupling configurations of network circuit.

3.2. Network Circuit

We constructed the network circuit from four unit circuits, connected to each other via capacitive coupling (**Fig.5**). The network dynamics are given by the following equations:

$$C\dot{V}_i^1 = -\frac{V_i^1}{R} + \frac{I_b}{2}F_\mu\left(\sum_{j,n} C_{i,j}^{1+,n}V_j^n - \sum_{j,n} C_{i,j}^{1-,n}V_j^n\right) \quad . \quad (12)$$

$$C\dot{V}_i^2 = -\frac{V_i^2}{R} + \frac{I_b}{2}F_\mu\left(\sum_{j,n} C_{i,j}^{2+,n}V_j^n - \sum_{j,n} C_{i,j}^{2-,n}V_j^n\right) \quad . \quad (13)$$

where V_i^1 and V_i^2 are the voltage of the first and second cell. The total capacitance of floating gate C_{T} is expressed by:

$$C_{\mathrm{T}} = C_{\mathrm{GD}} + C_{\mathrm{GS}} + C_{\mathrm{GB}} + \sum_{j,n} C_{i,j}^{m\pm,n} + C_{ctrl,i}^{m\pm,n} \quad . \quad . \quad (14)$$

where $C_{ctrl,i}^{m\pm,n}$ is the capacitance of each of the control gates, which is added to regulate the total capacitance of the floating-gate and connected to the grand potential.

During operation, the CPG network circuit generates different periodic patterns depending on its coupling configuration. **Fig.5** shows the coupling configurations that generate phase-locked oscillations that corresponds the typical locomotion patterns of mammals, such as walk, trot, and gallop.

Both state variables and interaction between cell circuits are expressed as voltage instead of current in the proposed circuit. Interactions are implemented via capacitive couplings. Consequently, the bias currents for stable operation can be reduced.

4. Simulation Results

In this section, we show the operation of the proposed circuit through computer simulation. In the following simulation, we used the circuit simulator HSPICE and MOSIS AMIS 1.5μm CMOS technology BSIM LEVEL 49 parameters. As typical device parameters, $\kappa = 0.6$ and $I_0 = 1.5 \times 10^{-16}$A were assumed. We detremined the design parameters of the circuit as follows: The aspect ratio of the MOS transistors $(W/L)_{\mathrm{n}} = (24\mu\mathrm{m}/8\mu\mathrm{m})$, $(W/L)_{\mathrm{p}} = (36\mu\mathrm{m}/8\mu\mathrm{m})$, where W and L are the gate width and length of the transistors, and n and p represent

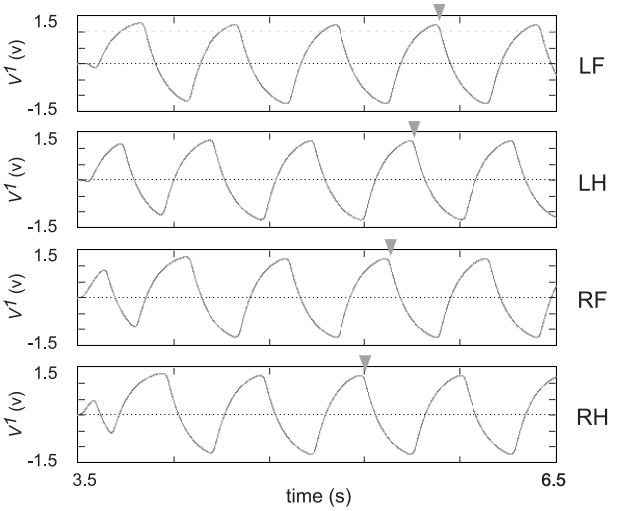

Fig. 6. Rhythmic pattern generation in walk mode.

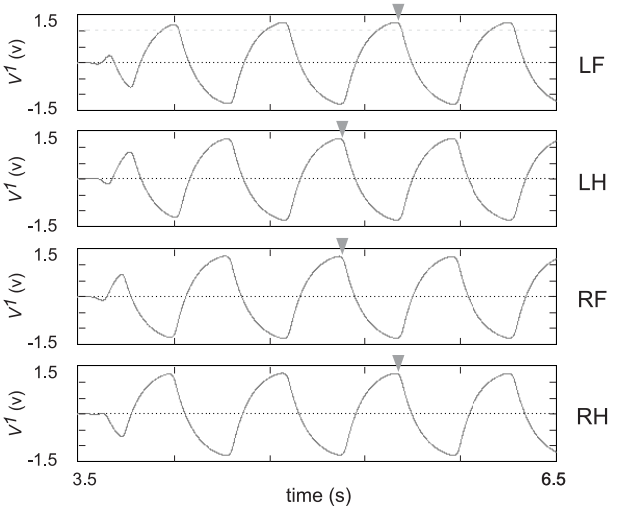

Fig. 7. Rhythmic pattern generation in trot mode.

n-channel and p-channel MOS transistors, capacitance $C = 20$nF, resistance $R = 6\mathrm{M}\Omega$, bias current $I_b = 500$nA, coupling capacitance

$$C_{i,i}^{1+,1} = C_{i,i}^{1-,2} = 0.5, \quad C_{i,i}^{2+,1} = 0.3, \quad C_T = 1.0\mathrm{pF},$$

and supply voltages $V_{\mathrm{DD}} = 1.5\mathrm{V}$ and $V_{\mathrm{SS}} = -1.5\mathrm{V}$.

4.1. Rhythmic Pattern Generation

First, we confirmed the rhythmic pattern generation in the network circuit. **Figs.6**-**8** show three examples of rhythmic patterns of voltage V_i^1 in the network circuit. It is shown that each rhythmic pattern corresponds to typical locomotion of mammals such as walk, trot, and gallop. Here, we assume that V_0^1, V_1^1, V_2^1 and V_3^1 drive the joints of the limbs LF, LH, RF, and RH as shown in **Fig.1**.

Figure 6 corresponds to the walk mode, in which we set the coupling capacitance at:

$$C_{0,2}^{1+,2} = C_{1,3}^{1+,2} = C_{2,1}^{1+,2} = C_{3,0}^{1+,2} = 0.2\mathrm{pF}$$

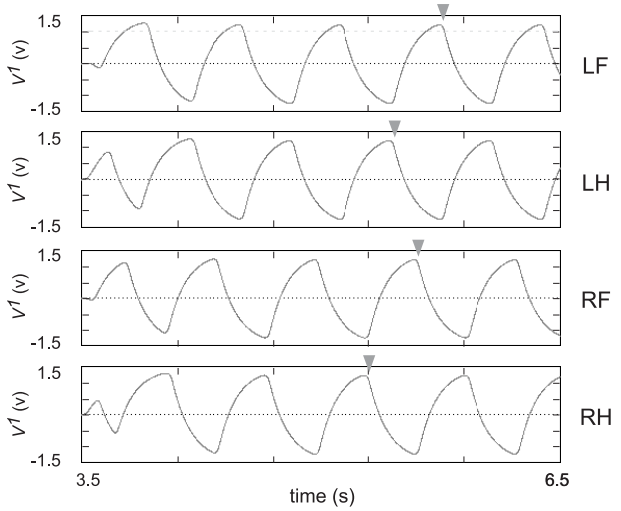

Fig. 8. Rhythmic pattern generation in gallop mode.

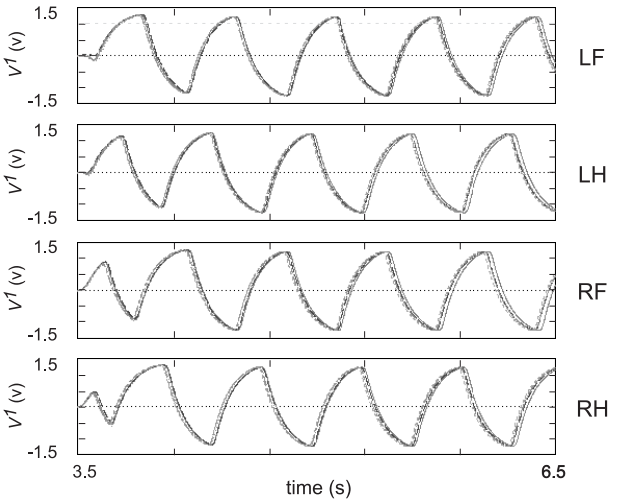

Fig. 10. Influence of capacitance mismatch on walk mode.

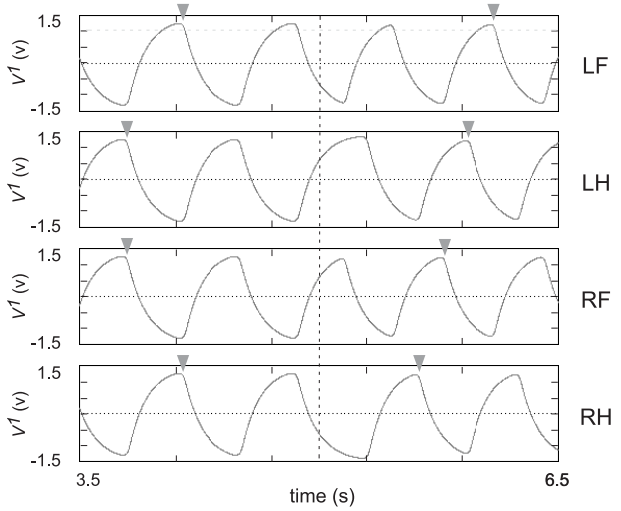

Fig. 9. Rhythmic pattern transition from trot to walk mode.

and others at 0F.

Figure 7 corresponds to the trot mode, in which we set the coupling capacitance at:

$$C_{0,3}^{1-,2} = C_{1,2}^{1-,2} = C_{2,1}^{1-,2} = C_{3,0}^{1-,2} = 0.1\text{pF}$$
$$C_{0,2}^{2-,2} = C_{1,3}^{2-,2} = C_{2,0}^{2-,2} = C_{3,1}^{2-,2} = 0.2\text{pF}$$

and others at 0F.

Figure 8 corresponds to the gallop mode, in which we set the coupling capacitance at:

$$C_{0,3}^{1+,2} = C_{1,0}^{1+,2} = C_{2,1}^{1+,2} = C_{3,2}^{1+,2} = 0.2\text{pF}$$

and others at 0F.

4.2. Rhythmic Pattern Transition

Second, we confirmed the transition between different rhythmic patterns in the network circuit. In the following, we changed the coupling configuration by switching the voltage connected to each input gate using multiplexers at 5.0s. **Fig.9** shows an example of transition in the circuit from trot to walk mode. In such a case, it is shown that the circuit can change the rhythmic patterns promptly.

4.3. Device Mismatch Influence

The device mismatch can adversely influence on circuit operation. Mismatch in a pair of transistors, for example, affect the current transfer ratio of the current mirror and the offset voltage of the differential pair. Such a mismatch is reduced by enlarging the size of transistors.

Mismatch in coupling capacitance may adversely affect rhythmic pattern generation in the network circuit. The device mismatch is usually characterized by standard deviations. Using the Monte-Carlo analysis, we studied the effects of mismatch in coupling capacitance, assuming that the coupling capacitances are implemented with the double polysilicon capacitors that achieve good matching performance. In the standard CMOS process, according to Gaussian distribution, matching accuracy in the double polysilicon capacitors is represented as $\sigma(\Delta C/C)$, where C is the average capacitance per unit area.

In the following, we estimate that $\sigma(\Delta C/C) = 0.1\%$. **Figs.10** and **11** show results from the Monte-Carlo analysis in both the trot and the walk mode operation (fifth iterations). These results show that the mismatch in coupling capacitance slightly affects the relative phases of phase-locked oscillation while it strongly affects transient response.

Through several computer simulations, we confirmed that the proposed circuit operated as predicted. First, we confirmed that the circuit produces different rhythmic patterns that correspond to locomotion patterns. Second, we confirmed that the circuit change its patterns promptly. Third, we confirmed the influence of device mismatch on circuit operation.

In our simulations, we considered only three coupling configurations, corresponding to walk, trot, and gallop modes. However, more interconnections between the unit

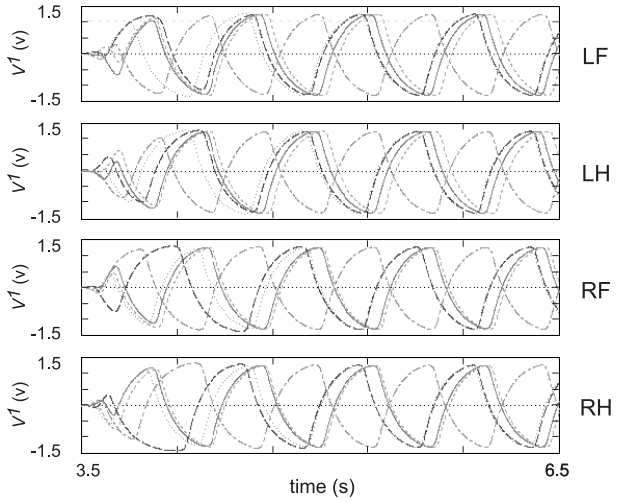

Fig. 11. Influence of capacitance mismatch on trot mode.

circuits, then more rhythmic patterns would be generated, thus, the proposed circuit is feasible as a CPG-based controller for rhythmic interlimb coordination in quadruped robot locomotion.

5. Summary

We proposed analog CMOS circuit implementation of a CPG-based controller for rhythmic interlimb coordination in quadruped robot locomotion. In previous works, proposed CPG-based locomotion controllers have mostly been implemented in software on digital microprocessors that processes only sequentially. Thus, increasing DOF of physical components of a robot deteriorates controllers performance. We designed a CPG-based controller as an analog CMOS circuit that processes in parallel essentially. We previously proposed analog CMOS circuit implementation of a CPG-based locomotion controller for a quadruped robot [12]. Our previous controller operates through current interaction, requiring that bias currents be controlled precisely to ensure that circuit operation is stable. To reduce bias currents for stable operation, we designed an analog CPG circuit using MIFG MOS transistors, aiming at voltage-mode operation.

A CPG-based locomotion controller for rhythmic interlimb coordination should generate different rhythmic patterns. Using the circuit simulator SPICE, we have shown that the circuit generates different patterns that correspond to typical locomotion patterns of mammals and changes its patterns promptly. Such circuit properties are sufficient for a CPG-based controller for a legged walking robot. Following present research, we are going to develop an autonomous quadruped walking robot.

Acknowledgements

The authors would like to thank Dr. M. Kitamura, Professor Emeritus of Hokkaido University, for his critical reading of the manuscript and his constructive comments and suggestions.

References:

[1] The 2nd International Symposium on Adaptive Motion of Animals and Machines, Kyoto, Japan, 2003.

[2] F. Delcomyn, "Neural basis of rhythmic behavior in animals," Science, Vol.210, pp. 492-498, 1980.

[3] F. Delcomyn, "Foundations of Neurobiology," New York: W, H. Freeman and Co., 1997.

[4] H. Kimura, Y. Fukuoka, and K. Konaga, "Adaptive Dynamic Walking of a Quadruped Robot by Using Neural System Model," Advanced Robotics, Vol.15, No.8, pp. 859-876, 2001.

[5] A. Billard, and A. J, Ijspeert, "Biologically inspired neural controllers for motor control in a quadruped walking robot," in IEEE-INNS International Joint Conference on Neural Networks, Italy, July 2000.

[6] H. Takemura, J. Ueda, Y. Matsumoto, and T. Ogasawara, "A Study of a Gait Generation of a Quadruped Robot Based on Rhythmic Control – Optimization of CPG Parameters by a Fast Dynamics Simulation Environment," in Proc. the Fifth International Conference on Climbing and Walking Robots, pp. 759-766, Paris, 2002.

[7] M. A. Lewis, M. J. Harttmann, R. Etienne-Cummings, and A. H. Cohen, "Control of a robot leg with an adaptive aVLSI CPG chip," Neurocomputing, Vol.38-40, pp. 1409-1421, 2001.

[8] M. Branciforte, G. Di Bernardo, F. Doddo, and L. Occhipinti, "Reaction-Diffusion CNN design for a new class of biologically-inspired processors in artificial locomotion applications," in Seventh International Conference on Microelectronics for Neural, Fuzzy and Bio-Inspired Systems, pp. 69-77, Granada, Spain, 1999.

[9] G. Brown, "On the nature of the fundamental activity of the nearvous centers: together with an anlysis of the conditioning of the rhythmic activity in progression, and a theory of the evoution of function in the nervoussystem," J. Physiol., Vol.48, pp. 18-46, 1914.

[10] G. Taga, Y. Yamaguchi, and H. Shimizu, "Self-organaized control of bipedal locomotion by neural oscillators in unpredictable environment," Biological Cybernetics, Vol.65, pp. 147-159, 1991.

[11] H. Nagashino, Y. Nomura, and Y. Kinouchi, "Generation and transitions of phase-locked oscillations in coupled neural oscillators," in the 40h SICE Annual Conference, Nagoya, Japan, 2001.

[12] K. Nakada, T. Asai, and Y. Amemiya, "An analog CMOS central pattern generator for interlimb coordination in quadruped locomotion," IEEE Tran. on Neural Networks, Vol.14, No.5, pp. 1356-1365, 2003.

[13] H.R. Wilson, and J.D. Cowan, "Excitatory and inhibitory interactions in localized populations of model neurons," Biophys. J., Vol.12, pp. 1-24, 1972.

[14] T. Ueta, and G. Chen, "On synchronization and control of coupled Wilson-Cowan neural oscillators," International Journal of Bifurcation and Chaos, Vol.13, No.1, pp. 163-175, 2003.

[15] F. C. Hoppensteadt, and E. M. Ihnikevich, "Weakly connected neural networks," Springer, Heidelberg, 1997.

[16] C. A. Mead, "Analog VLSI and neural systems," Addison-Wesley, Reading, 1989.

[17] M. Isami, and T. Fiez, Eds. "Analog VLSI: Signal and Information Processing," McGraw-Hill, 1993.

[18] R. J. Barker, H. W. Li, and D. E. Boyce, "CMOS circuit design, layout, and simulation," IEEE Press, 1998.

[19] T. Shibata, and T. Ohmi, "A functional MOS transistor featuring gate level weighted sum and threshold operations," IEEE, Trans. on Electron Devices, Vol.39, No.6, pp. 1444-1445, 1990.

[20] B. A. Minch, C. Diorio, P. Hasler, and C. A. Mead, "Translinear circuits using subthreshold floating-gate MOS transistors," Analog Integrated Circuits and Signal Processing, Vol.9, No.2, pp. 167-179, 1998.

Name:
Kazuki Nakada

Affiliation:
Ph.D. Student, Department of Electrical Engineering, Hokkaido University

Address:
Kita 13, Nishi 8, Sapporo 060-8628, Japan

Brief Biographical History:
2002- Working toward the D. E. degree at Hokkaido University

Main Works:
• "An analog CMOS central pattern generator for interlimb coordination in quadruped locomotion," IEEE Transaction on Neural Networks, Vol.14, No.5, pp. 1356-1365, 2003.

Membership in Learned Societies:
• The Institute of Electrical and Electronics Engineers (IEEE)
• Japanese Neural Network Society (JNNS)

Name:
Yoshihito Amemiya

Affiliation:
Professor, Department of Electrical Engineering, Hokkaido University

Address:
Kita 13, Nishi 8, Sapporo 060-8628, Japan

Brief Biographical History:
1975- NTT Electrical Communication Laboratories
1993- Full Professor at Hokkaido University

Main Works:
• "Quantum-dot logic circuits based on the shred binary-decision diagram," Jpn. J. Appl. Phys., Vol.40, No.7, pp. 4485-4488, 2001.

Membership in Learned Societies:
• The Institute of Electronics, Information and Communication Engineers (IEICE)
• The Institute of Electrical Engineers of Japan

Name:
Tetsuya Asai

Affiliation:
Associate Professor, Department of Electrical Engineering, Hokkaido University

Address:
Kita 13, Nishi 8, Sapporo 060-8628, Japan

Brief Biographical History:
1999- Research Associate at Hokkaido University
2001- Associate Professor at Hokkaido University

Main Works:
• "Towards reaction-diffusion computing devices based on minority-carrier transport in semiconductors," Chaos, Solitons & Fractals, Vol.20, No.4, pp. 863-876, 2004.

Membership in Learned Societies:
• The Institute of Electrical and Electronics Engineers (IEEE)
• Japanese Neural Network Society (JNNS)
• The Japan Society of Applied Physics (JSAP)